STABILIZATION OF SAWTOOTH OSCILLATION BY ISLAND HEATING

W. Park, D. A. Monticello, and T. K. Chu

Plasma Physics Laboratory, Princeton University

P.O. Box 451

Princeton, NJ 08544

PPPL--2385

DE87 003075

ABSTRACT

Using the compressible resistive MHD equations in a finite aspect ratio cylinder, it is found that the m = 1 mode (the sawtooth oscillation) can saturate when the pressure inside the magnetic island is higher than that of the original core plasma. The saturation condition is of the form $\Delta\beta_p \gtrsim 8\,\varepsilon_{q=1}^{-1}\,(1 - q_0)^2$. This saturation effect can be used to actively stabilize sawteeth by heating the island and/or by cooling the core plasma. This mechanism together with a stabilizing toroidal effect may also explain recent lower-hybrid-wave-driven tokamak experiments where the saturation of sawteeth has been observed.

MASTER

EbB

DISTRIBUTION OF THIS DOCUMENT IS UNLIMITED

Sawtooth oscillation[1] in tokamaks degrades pressure confinement inside the safety factor q = 1 surface, and limits the central q_c to be close to unity. Suppression of sawteeth should give marked improvement in tokamak performance including better stability for $m \geq 2$ modes and better confinement times. However, the m = 1 mode which is responsible for the sawtooth crash has been found to be more difficult to stabilize than $m \geq 2$ modes.[2] Unlike $m \geq 2$ modes, which grow nonlinearly on a slow resistive time scale τ_η,[3,4] the nonlinear m = 1 mode (sawtooth crash) is driven by ideal free energy and grows on a much faster hybrid time scale $(\tau_\eta^{1/2}\ \tau_A^{1/2})$, where τ_A is the Alfvén time.[4] The reason for this fast time scale is the fact that the island equilibrium for the m = 1 modes contains a singular current spike at the x-point as shown in Fig. 1.[4] This should be contrasted with nonlinear $m \geq 2$ modes which go through a succession of regular equilibrium states.[3,4]

Remembering that $m \geq 2$ modes are linearly stable to ideal modes, one may expect that if the m = 1 mode can be made stable to ideal linear modes, the nonlinear m = 1 mode may behave as nonlinear $m \geq 2$ modes, i.e., showing a slow nonlinear growth and saturation. This turns out to be the case as long as the linear stability is robust enough.[5] Otherwise, the ideal driving free energy comes in nonlinearly even when linearly stable. From the equation for the ideal linear growth rate of the m = 1 mode,

$$\gamma = K \int_0^s \left\{-2\ \varepsilon^2 r^2\ \frac{\partial P}{\partial r} + \varepsilon^2 r B_\theta^2\ (3\ q + 1)\ (1 - q)\right\} dr \qquad , \tag{1}$$

where r = s is the position of the q = 1 surface, one can see there are two ways to make the mode stable ($\gamma < 0$). One way is to have the q-profile rise inside the q = 1 surface as in reversed-field pinches. The other is to invert

NOTICE

This report was prepared as an account of work sponsored by the United States Government. Neither the United States nor the United States Department of Energy, nor any of their employees, nor any of their contractors, subcontractors, or their employees, makes any warranty, express or implied, or assumes any legal liability or responsibility for the accuracy, completeness or usefulness of any information, apparatus, product or process disclosed, or represents that its use would not infringe privately owned rights.

Printed in the United States of America

Available from:

National Technical Information Service
U.S. Department of Commerce
5285 Port Royal Road
Springfield, Virginia 22161

Price Printed Copy $ ___*___; Microfiche $4.50

*Pages	NTIS Selling Price
1-25	$7.00
25-50	$8.50
51-75	$10.00
76-100	$11.50
101-125	$13.00
126-150	$14.50
151-175	$16.00
176-200	$17.50
201-225	$19.00
226-250	$20.50
251-275	$22.00
276-300	$23.50
301-325	$25.00
326-350	$26.50
351-375	$28.00
376-400	$29.50
401-425	$31.00
426-450	$32.50
451-475	$34.00
476-500	$35.50
500-525	$37.00
526-550	$38.50
551-575	$40.00
567-600	$41.50

For documents over 600 pages, add $1.50 for each additional 25-page increment.

the pressure profile so that $P_{center} < P_{q=1}$. (Recently it was reported that when incompressible MHD codes were used, saturation of the m = 1 mode occurred.[6,7] However, the incompressibility assumption generates an inverted pressure profile even when the initial pressure is zero in the calculation.[8] This inverted pressure gives a saturation as discussed above. With the present compressible code with initial zero pressure, no saturation occurred.)

In this report, we generalize this stabilizing effect to include the magnetic island in nonlinear development. We find that pressure has the opposite effect on stability inside the island compared to the effect inside the initial core plasma, i.e., a peaked pressure gives stability while an inverted pressure gives instability. The total effect of pressure inside both the plasma core and the island can be approximated by $\Delta\beta_p$ where

$$\Delta\beta_p \equiv (P_I - P_c)/(B_{\theta,q=1}^2/2) \quad .$$

Here P_I is the pressure at the center of the island and P_c is the pressure at the original magnetic axis. $\Delta\beta_p > 0$ gives stability. An example of a saturated m = 1 mode with $\Delta\beta_p = 0.25$ is shown in Fig. 2. Figure 2(a) and (b) show the pressure profile which is peaked inside the island. Figure 2(c) shows the flux ψ contours. Figure 2(d) shows the toroidal current density J_Z profile along the midplane. Note that no current spike exists in the current profile, indicating a regular equilibrium state in contrast to the case shown in Fig. 1(b). The state had an initial q-profile of $q = q_o\,[1 + (r/c)^2]$ with $q_o = 0.95$, $r_{q=1} = 0.5$, and $\varepsilon = 0.2$.

When we keep the pressure profile the same while reducing q_o further, the state became unstable and went through a complete fast reconnection. From a series of such studies with different pressure profiles and $\varepsilon_{q=1}$, we find the saturation condition between $\Delta\beta_p$ and q_o as

$$\Delta\beta_p \gtrsim 8\ \epsilon_{q=1}^{-1}\ (\Delta q)^2, \tag{2}$$

where $\Delta q = 1-q_o$ and $\epsilon_{q\ =\ 1}$ is the inverse aspect ratio at the q = 1 surface.

The saturation condition, Eq. (2), can be used to actively stabilize sawteeth by heating the island and/or by cooling the original plasma core using pellet injection. In this scheme the condition (2) has to be satisfied continuously. This is possible because $\Delta\beta_p$ only has to be increased as $\Delta q = 1 - q_o$ increases, which changes on a slow resistive time scale. The required $\Delta\beta_p$ is in a practical range in high β tokamaks. For example, to stabilize down to $q_o = 0.9$, $\Delta\beta_p = 0.8$ with $\epsilon_{q\ =\ 1} = 0.1$ is required. This will give saturation until q_o goes below 0.9.

The stabilization effect studied above can be also used to explain recent lower-hybrid-wave-driven tokamak experiments[10] where saturation of sawteeth has been observed. Experimental ECE signals suggest that the island is heated effectively, and at an input power level where the saturation of sawteeth occurs, the island temperature reaches close to that of the peak temperature at the original axis. This will give $\Delta\beta_p \approx 0$ and hence no saturation from the condition (2). However, we have to take into account a toroidal stabilization effect which we neglected in our cylindrical model. If we assume that toroidal effects give saturation of the m = 1 mode up to $\Delta q \approx \delta$ in the absence of the island heating where δ is a small positive number, the island heating effect can be estimated to give saturation up to $\Delta q = \delta + (\epsilon_{q\ =\ 1}\ \Delta\beta_{pI}/8)^{1/2} \approx \delta + 0.05$. Here $\Delta\beta_{pI} \approx 0.2$ and $\epsilon_{q\ \approx\ 1} = 0.08$ is estimated from the experimental data. The sawtooth crash will be stabilized until $q_o = 0.95-\delta$ is reached. This time can be estimated as $\tau \approx \Delta q(T/\Delta T)\ (a_{q\ =\ 1}^2/\eta) \approx 100$ msec. Here the amplitude of the temperature oscillation $\Delta T/T \approx 0.2$ is used. This can explain the saturation phenomena in PLT experiments. There is substantial uncertainty in the estimate of $\Delta\beta_p$. However, changing to $\Delta\beta_p = 0.05$ still gives a reasonable time scale of $\tau = 50$ msec.

The overall picture in this model is the following. As q_0 drops below one, the resistive mode is destabilized, but the ideal mode does not enter either linearly or nonlinearly until q_0 reaches $1 - \delta$. During this time, an island will form on a slow resistive time scale and will be heated by lower hybrid wave. q_0 drops further while the island heating keeps the stability condition (2) continuously satisfied until $q_0 = 0.95-\delta$ is reached. One factor which may help the preferential heating of the island is the fact that the shear inside the island is usually lower than that of the main plasma core. This makes it harder to destroy good flux surfaces inside the island compared to the main plasma core. The toroidal effect we assumed here is far from certain. The curvature of the magnetic field, which determines the stability character of a given pressure profile, is quite different in a torus compared to a cylinder. In a complicated geometry of the nonlinear phase, how the toroidicity affects stability is not clearly known. This question will be studied using a three-dimensional code.

The above model does not completely explain the total elimination of the $m = 1$ mode found in the PLT lower hybrid wave experiments with even higher wave power. However, whether the $q = 1$ surface actually lies inside the plasma in this case is not clearly answered in the experiment. In our study, we have also neglected the fact that lower hybrid waves also drive plasma current such that the usual Ohm's law may have to be changed significantly and that a large portion of the plasma current is due to runaway electrons.

In the above study we have used the MH2D code which solves compressible helical MHD equations in the finite aspect ratio cylinder. The compressibility is added into the incompressible IMH2D code.[4,10] (The reduced two-dimensional tokamak equations[11] which approximate a tokamak as an infinite aspect ratio cylinder are not applicable to the present case because these equations do not include compressibility and pressure effects.) The equations we use are described in the following.

In helical symmetry, all variables are functions of (r,ϕ) where the helical angle $\phi = \theta + \alpha z$ with helicity α and with the usual cylindrical coordinates (r,θ,z). We use basis vectors $(\hat{r},\hat{\phi},\hat{e})$ where $\hat{r} = \nabla r$, $\hat{\phi} = \nabla\phi/|\nabla\phi|$, and $\hat{e} = \hat{r} \times \hat{\phi}$. Then, the magnetic field and the velocity can be represented as

$$\vec{B} = g\nabla\psi \times \hat{e} + B_e\hat{e} \quad ,$$

$$\vec{V} = g\nabla U \times \hat{e} + V_e\hat{e} + \nabla\chi \quad ,$$

where $g \equiv (1 + \alpha^2 r^2)^{-1/2}$.

The helical compressible MHD equations with a scalar resistivity η are (in rationalized emu units)

$$\frac{d\psi}{dt} = -\frac{\eta J_e}{g} \; ,$$

$$\left(\frac{d}{dt}\right)(\Delta^{\dagger}U) = -\vec{B}\cdot\nabla(gJ_e) + gW_e\nabla^2\chi + \alpha^2 g^2\left[\frac{\partial(V_e^2 - B_e^2)}{\partial\phi}\right] - 2\alpha\vec{V}\cdot\nabla(g^3 V_e) \quad ,$$

$$\left(\frac{d}{dt}\right)(gB_e) = \vec{B}\cdot\nabla(gV_e) - g\,B_e\nabla^2\chi + 2\alpha g^4\vec{V}\cdot\nabla\psi + \left\{\nabla\cdot\left[g^2\eta\nabla\left(\frac{B_e}{g}\right)\right] + \eta(2\alpha g^3)J_e\right\} \; ,$$

$$\left(\frac{d}{dt}\right)\left(\frac{V_e}{g}\right) = \vec{B}\cdot\nabla\left(\frac{B_e}{g}\right) \quad , \qquad (3)$$

$$\frac{\partial\nabla^2\chi}{\partial t} + \frac{1}{2}\nabla^2\left(g^2\,\nabla u\cdot\nabla u + V_e^{\,2} + 2\nabla\chi\times g\,\nabla u\cdot\hat{e} + \nabla\chi\cdot\nabla\chi\right)$$

$$+ \nabla\chi\times g\nabla\left(\frac{W_e}{g}\right)\cdot\hat{e}$$

$$= -\nabla\cdot\left(gW_e\nabla u - gV_e\,\nabla\left(\frac{V_e}{g}\right)\right)$$

$$+ \nabla\cdot\left(gJ_e\,\nabla\Psi - g\,B_e\,\nabla\left(\frac{B_e}{g}\right)\right) - \nabla^2 p \quad ,$$

$$\frac{dp}{dt} = -\gamma\,p\,\nabla^2\chi + \nabla\cdot[\kappa\cdot\nabla p] + S_p \quad .$$

Here,

$$\nabla f = \left(\frac{\partial f}{\partial r}\right)\nabla r + \left(\frac{\partial f}{\partial\phi}\right)\nabla\phi = \left(\frac{\partial f}{\partial r}\right)\hat{r} + \left(\frac{1}{rg}\right)\left(\frac{\partial f}{\partial\phi}\right)\hat{\phi} \quad ,$$

$$\Delta^\dagger f \equiv \nabla\cdot\left(g^2\nabla f\right) = \left(\frac{1}{r}\right)\left[\left(\frac{\partial}{\partial r}\right)\left(\frac{rg^2\partial f}{\partial r}\right)\right] + \left(\frac{1}{r^2}\right)\left(\frac{\partial^2 f}{\partial\phi^2}\right) \quad ,$$

$$J_e = -\left(\Delta^\dagger\psi/g + 2\alpha g^2 B_e\right),\; W_e = -\left(\Delta^\dagger U/g + 2\alpha g^2\,V_e\right),\; \vec{V}\cdot\nabla f = \left(\nabla f\times g\nabla U\right)\cdot\hat{e} + \nabla\chi\cdot\nabla f \quad ,$$

$$\vec{B}\cdot\nabla f = \left(\nabla f\times g\nabla\psi\right)\cdot\hat{e} \quad ,$$

and

$$d/dt = \partial/\partial t + V\cdot\nabla.$$

In the above equations, we assumed an appropriate density source S_ρ in the density equation (i.e., $\partial\rho/\partial t = -\,\mathrm{div}\,(\rho\vec{V}) + S_\rho$) such that $\rho = 1$ always. Such a density source will somewhat change the time scales of local phenomena, but not the overall physics. This approximation significantly reduces the complexity of the equations and also greatly enhances the numerical accuracy of the calculation. The heat conduction term is not solved by a direct method because the large $\kappa_{\parallel}$ ($\kappa_{\parallel} \gg \kappa_{\perp}$) causes a large numerical error. Instead this term is solved using the artificial parallel velocity method described in Ref. 12. This gives the $B \cdot \nabla p = 0$ condition in an efficient way. By setting $\chi \equiv 0$ in the above equations, the incompressible helical MHD equations[4,10] can be obtained.

We wish to thank Drs. A. H. Boozer, K. McGuire, P. H. Rutherford, and R. B. White for helpful discussions. This work was supported by the U. S. Department of Energy Contract No. DE-AC02-76CHO3073.

REFERENCES

[1]S. von Goeler, W. Stodiek, and N. Sauthoff, Phys. Rev. Lett. 33, 1201 (1974).

[2]R.B. White, P.H. Rutherford, H.P. Furth, W. Park, and L. Chen, in Magnetic Reconnection and Turbulence, M. Dubois et al. Eds. (Editions de Physique, Orsay, 1985) p. 299.

[3]P.H. Rutherford, Phys. Fluids 16, 1903 (1973).

[4]W. Park, D.A. Monticello, and R.B. White, Phys. Fluids 27, 137 (1984).

[5]W. Park, D.A. Monticello, Sherwood Meeting on Theoretical Aspects of Thermo. Nucl. Res., Madison Wisconsin (1985) 1C5.

[6]Y. Tanaka, M. Azumi, G. Kurita, and T. Takeda, Plasma Phys. Controlled Fusion 27, 590 (1985).

[7]L.A. Charlton, B.A. Carreras, T. Hender, H.R. Hicks, J.A. Holmes, and V.E. Lynch, Bull. Am. Phys. Soc. 30, 1479 (1985).

[8]W. Park and D.A. Monticello, Sherwood Meeting on Theoretical Aspects of Thermo. Nucl. Res., New York, NY (1986) 1C19.

[9]T.K. Chu et al., Nucl. Fusion 26, 666 (1986).

[10]W. Park, D.A. Monticello, R.B. White, and S.C. Jardin, Nucl. Fusion 20, 1181 (1980).

[11]M.N. Rosenbluth, D.A. Monticello, H.R. Strauss, and R.B. White, Phys. Fluids 19, 1987 (1976).

[12]W. Park, D.A. Monticello, H.R. Strauss, and J. Manickam, Phys. Fluids 29, 1171 (1986).

FIGURE CAPTIONS

Fig. 1 Plasma profiles during a fast reconnection, (a) helical flux contours, and (b) toroidal current profile along the midplane. At the x-point, $J_z \to \infty$ as $\eta \to 0$.

Fig. 2 A saturated state with $\Delta\beta_p \simeq 0.25$. (a) and (b) show the pressure profile which is peaked inside the island. (c) is the helical flux contours and (d) the toroidal current profile along the midplane. Note that no current spike exists in the current profile.

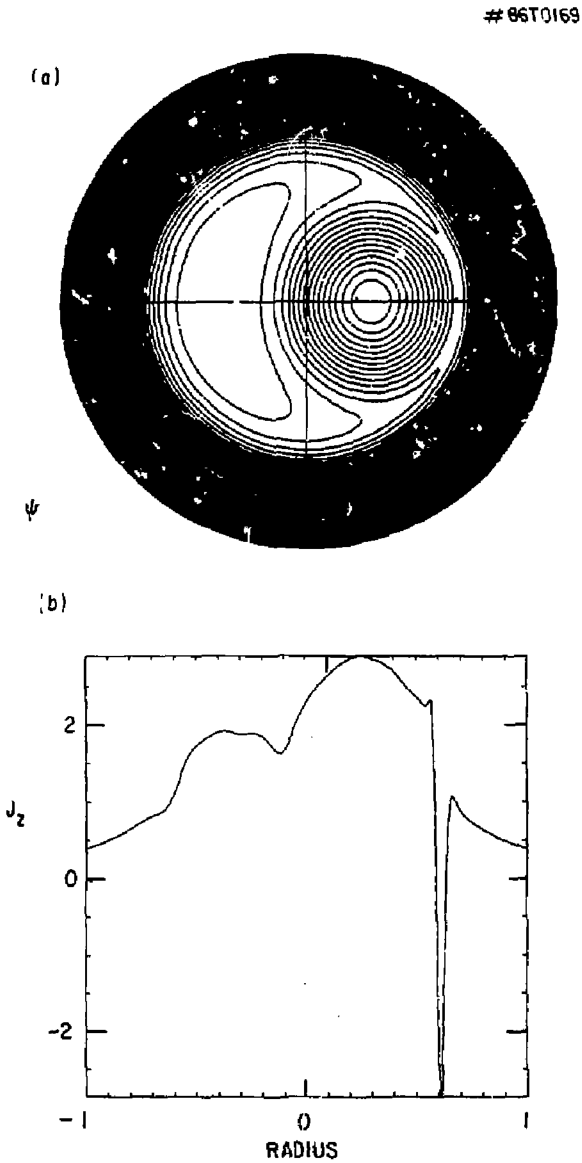

Fig. 1

#86T0170

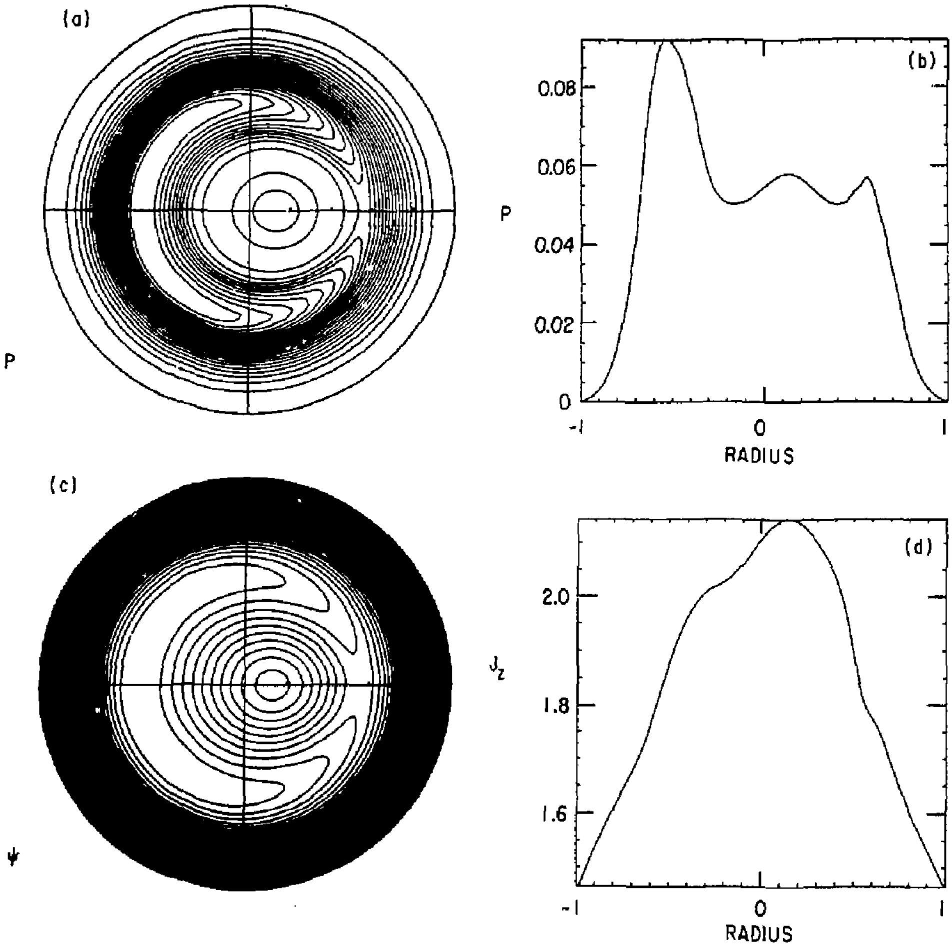

Fig. 2

EXTERNAL DISTRIBUTION IN ADDITION TO UC-20

Plasma Res Lab, Austra Nat'l Univ, AUSTRALIA
Dr. Frank J. Paoloni, Univ of Wollongong, AUSTRALIA
Prof. I.R. Jones, Flinders Univ., AUSTRALIA
Prof. M.H. Brennan, Univ Sydney, AUSTRALIA
Prof. F. Cap, Inst Theo Phys, AUSTRIA
M. Goossens, Astronomisch Instituut, BELGIUM
Prof. R. Boucique, Laboratorium voor Natuurkunde, BELGIUM
Dr. D. Palumbo, Dg XII Fusion Prog, BELGIUM
Ecole Royale Militaire, Lab de Phys Plasmas, BELGIUM
Dr. P.H. Sakanaka, Univ Estadual, BRAZIL
Lib. & Doc. Div., Instituto de Pesquisas Espaciais, BRAZIL
Dr. C.R. James, Univ of Alberta, CANADA
Prof. J. Teichmann, Univ of Montreal, CANADA
Dr. H.M. Skarsgard, Univ of Saskatchewan, CANADA
Prof. S.R. Sreenivasan, University of Calgary, CANADA
Prof. Tudor W. Johnston, INRS-Energie, CANADA
Dr. Hannes Barnard, Univ British Columbia, CANADA
Dr. M.P. Bachynski, MPB Technologies, Inc., CANADA
Chalk River, Nucl Lab, CANADA
Zhengwu Li, SW Inst Physics, CHINA
Library, Tsing Hua University, CHINA
Librarian, Institute of Physics, CHINA
Inst Plasma Phys, Academia Sinica, CHINA
Dr. Peter Lukac, Komenskeho Univ, CZECHOSLOVAKIA
The Librarian, Culham Laboratory, ENGLAND
Prof. Schatzman, Observatoire de Nice, FRANCE
J. Radet, CEN-BP6, FRANCE
JET Reading Room, JET Joint Undertaking, ENGLAND
AM Dupas Library, AM Dupas Library, FRANCE
Dr. Tom Mual, Academy Bibliographic, HONG KONG
Preprint Library, Cent Res Inst Phys, HUNGARY
Dr. R.K. Chhajlani, Vikram Univ, INDIA
Dr. B. Dasgupta, Saha Inst, INDIA
Dr. P. Kaw, Physical Research Lab, INDIA
Dr. Phillip Rosenau, Israel Inst Tech, ISRAEL
Prof. S. Cuperman, Tel Aviv University, ISRAEL
Prof. G. Rostagni, Univ Di Padova, ITALY
Librarian, Int'l Ctr Theo Phys, ITALY
Miss Clelia De Palo, Assoc EURATOM-ENEA, ITALY
Biblioteca, del CNR EURATOM, ITALY
Dr. H. Yamato, Toshiba Res & Dev, JAPAN
Direc. Dept. Lg. Tokamak Dev, JAERI, JAPAN
Prof. Nobuyuki Inoue, University of Tokyo, JAPAN
Research Info Center, Nagoya University, JAPAN
Prof. Kyoji Nishikawa, Univ of Hiroshima, JAPAN
Prof. Sigeru Mori, JAERI, JAPAN
Prof. S. Tanaka, Kyoto University, JAPAN
Library, Kyoto University, JAPAN
Prof. Ichiro Kawakami, Nihon Univ, JAPAN
Prof. Satoshi Itoh, Kyushu University, JAPAN
Dr. D.I. Choi, Adv. Inst Sci & Tech, KOREA
Tech Info Division, KAERI, KOREA
Bibliotheek, Fom-Inst Voor Plasma, NETHERLANDS
Prof. B.S. Liley, University of Waikato, NEW ZEALAND
Prof. J.A.C. Cabral, Inst Superior Tecn, PORTUGAL
Dr. Octavian Petrus, ALI CUZA University, ROMANIA
Prof. M.A. Hellberg, University of Natal, SO AFRICA
Dr. Johan de Villiers, Plasma Physics, Nucor, SO AFRICA
Fusion Div. Library, JEN, SPAIN
Prof. Hans Wilhelmson, Chalmers Univ Tech, SWEDEN
Dr. Lennart Stenflo, University of UMEA, SWEDEN
Library, Royal Inst Tech, SWEDEN
Centre de Recherchesen, Ecole Polytech Fed, SWITZERLAND
Dr. V.T. Tolok, Kharkov Phys Tech Ins, USSR
Dr. D.D. Ryutov, Siberian Acad Sci, USSR
Dr. G.A. Eliseev, Kurchatov Institute, USSR
Dr. V.A. Glukhikh, Inst Electro-Physical, USSR
Institute Gen. Physics, USSR
Prof. T.J.M. Boyd, Univ College N Wales, WALES
Dr. K. Schindler, Ruhr Universitat, W. GERMANY
ASDEX Reading Rm, IPP/Max-Planck-Institut für Plasmaphysik, F.R.G.
Nuclear Res Estab, Julich Ltd, W. GERMANY
Librarian, Max-Planck Institut, W. GERMANY
Bibliothek, Inst Plasmaforschung, W. GERMANY
Prof. R.K. Janev, Inst Phys, YUGOSLAVIA